Synthesis and Properties of a Conformationally Restricted Spin-Labeled Analog of ATP and Its Interaction with Myosin and Skeletal Muscle†

Dario R. Alessi,‡ John E. T. Corrie,§ Piotr G. Fajer,∥,⊥ Michael A. Ferenczi,§ David D. Thomas,∥ Ian P. Trayer,*,‡ and David R. Trentham§

School of Biochemistry, The University of Birmingham, Edgbaston, Birmingham B15 2TT, U.K., National Institute for Medical Research, The Ridgeway, Mill Hill, London NW7 1AA, U.K., and Department of Biochemistry, University of Minnesota Medical School, Minneapolis, Minnesota 55455

Received February 13, 1992; Revised Manuscript Received May 26, 1992

ABSTRACT: The synthesis is described of a spin-labeled analog of ATP, 2′,3′-*O*-(1-oxy-2,2,6,6-tetramethyl-4-piperidylidene)adenosine 5′-triphosphate (SL-ATP). The spin-label moiety is attached by two bonds to the ribose ring as a spiroketal and hence has restricted conformational mobility relative to the ribose moiety of ATP. The synthesis proceeds via an acid-catalyzed addition of adenosine 5′-monophosphate to 1-acetoxy-4-methoxy-2,2,6,6-tetramethyl-1,2,5,6-tetrahydropyridine in acetonitrile. The spiroketal product is pyrophosphorylated, and alkaline hydrolysis with concomitant aerial oxidation gives the required product. The spin-labeled moiety probably takes up two rapidly interconverting conformations with respect to the ribose ring on the basis of the ^{1}H NMR spectra of its precursors and related uridine derivatives [Alessi et al. (1991) *J. Chem. Soc., Perkin Trans. 1*, 2243–2247]. SL-ATP is a substrate for myosin and actomyosin with similar kinetic parameters to ATP during triphosphatase activity. SL-ATP supports muscle contraction and permits relaxation of permeabilized rabbit skeletal muscle fibers. SL-ADP is a substrate for yeast 3-phosphoglycerate kinase, thus permitting regeneration of SL-ATP from SL-ADP within muscle fibers. Electron paramagnetic resonance (EPR) studies of SL-ADP bound to myosin filaments and to myofibrils show a degree of nanosecond motion independent of that of the protein, which may be due to conformational flexibility of the ribose moiety of ATP bound to myosin's active site. This nanosecond motion is more restricted in myofibrils than in myosin filaments, suggesting that the binding of actin affects the ribose binding site in myosin. EPR studies on SL-ADP bound to rigor cross-bridges in muscle fiber bundles showed the nucleotide to be highly oriented with respect to the fiber axis.

Many problems in biology are related to the dynamics, structure, and orientation of macromolecules. Nitroxyl spin-labeled probes have been of value in addressing these issues by EPR spectroscopy (Thomas, 1987) and NMR spectroscopy (Kosen, 1989). A difficulty when such probes are introduced directly onto macromolecules in either organized cellular or purified preparations is that of specificity (Seidel, 1982). One solution is to label smaller molecules such as enzyme substrates (Roberts et al., 1969) that interact with specific sites on macromolecules, while another has been covalently to attach a nitroxyl label to a specific site on the protein (Thomas & Cooke, 1980). A further problem in the spin-label technique is that a nitroxyl probe may have mobility independent of the macromolecule to which it is attached and whose properties are to be analyzed. An approach to solving these problems is to utilize an enzyme substrate that binds tightly to its protein and is thus likely to have restricted motion with respect to the macromolecule and for the EPR probe in turn to have restricted motion relative to the remainder of the substrate.

With these considerations in mind, we set out to synthesize an analog of ATP containing a nitroxide spin label whose motion is severely restricted with respect to the ribose moiety of ATP. We chose to attach the probe by two covalent bonds to the ribose ring of ATP to form SL-ATP,[1] the spin-labeled spiroketal **5** (Scheme I). Such a probe might be expected to be useful in analyzing the motion and orientation of cross-bridges in muscle, since the myosin ATPase site has a high affinity for ATP (Mannherz et al., 1974) and other ribose-modified ATP analogs (Crowder & Cooke, 1987). Furthermore, ribose-modified ATP analogs are effective substrates for myosin and actomyosin and support muscular contraction, e.g., MantATP (Woodward et al., 1991).

Several difficulties were encountered in the synthesis of SL-ATP. Many of these were addressed or bypassed in a synthesis of the corresponding uridine analog (Alessi et al., 1991). Two problems overcome here are the lability of the ribose–purine bond during the acid-catalyzed introduction of the spin-label precursor onto ribose (first reaction in Scheme I) and the insolubility of the nucleotide (as opposed to de-

* Author to whom correspondence should be addressed.

† This work was supported by the Wellcome Trust, the Science and Engineering Research Council, U.K., the Medical Research Council, U.K., the Muscular Dystrophy Association, and Grant HL 15835 from the National Institutes of Health.

‡ The University of Birmingham.
§ National Institute for Medical Research.
∥ University of Minnesota Medical School.
⊥ Present address: Department of Biological Science, Florida State University, Tallahassee, FL 32306.

[1] Abbreviations: SL-ATP (ADP), spin-labeled ATP (ADP); DMF, *N*,*N*-dimethylformamide; PGK, 3-phospho-D-glycerate kinase; GAP-DH, D-glyceraldehyde-3-phosphate dehydrogenase; NADH, reduced nicotinamide adenine dinucleotide; NAD^+, nicotinamide adenine dinucleotide; P_i, inorganic phosphate; S1(A1), chymotryptic myosin subfragment 1 with the A1 light chain; TEA, triethanolamine; TEAB, triethylammonium bicarbonate; TES, *N*-[tris(hydroxymethyl)methyl]-2-aminoethanesulfonic acid; MeOH, methanol; HPLC, high-pressure liquid chromatography; EPPS, 4-(2-hydroxyethyl)-1-piperazine-3-propanesulfonic acid.

0006-2960/92/0431-8043$03.00/0

Scheme I: Synthesis of 2′,3′-*O*-(1-Oxy-2,2,6,6-tetramethyl-4-piperidylidene)adenosine 5′-Triphosphate (SL-ATP)[a]

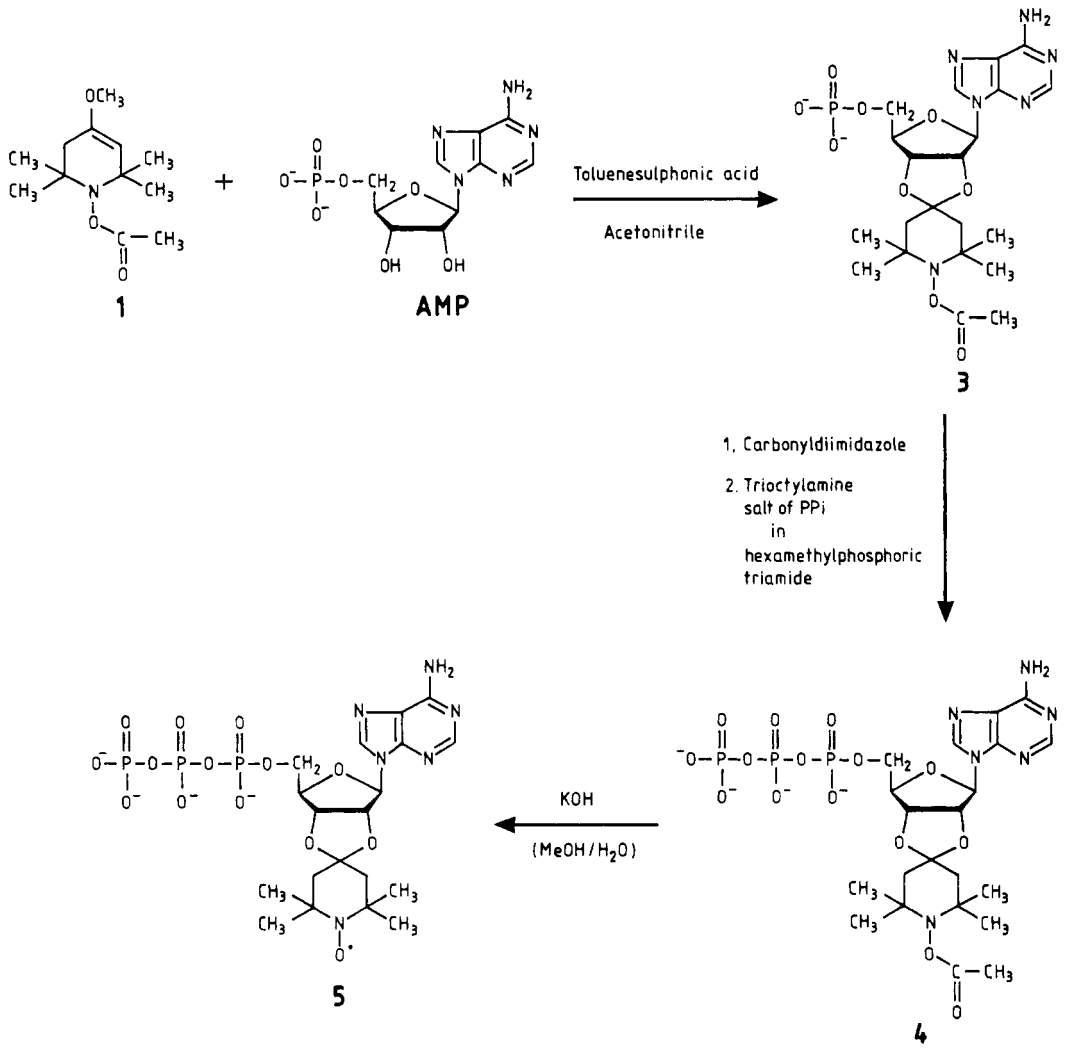

[a] Charges are drawn as for pH 7. The actual ionization states depend on reaction conditions. The preparation of the enol ether **1** (1-acetoxy-4-methoxy-2,2,6,6-tetramethyl-1,2,5,6-tetrahydropyridine) is described in Alessi et al. (1991). Subsequent details of the condensation of **1** with AMP to form **3** [2′,3′-*O*-(1-acetoxy-2,2,6,6-tetramethyl-4-piperidylidene)adenosine 5′-monophosphate], its pyrophosphorylation to form **4** [2′,3′-*O*-(1-acetoxy-2,2,6,6-tetramethyl-4-piperidylidene)adenosine 5′-triphosphate], and its deacylation and aerial oxidation to form **5** [2′,3′-*O*-(1-oxy-2,2,6,6-tetramethyl-4-piperidylidene)adenosine 5′-triphosphate] are given under Experimental Procedures.

rivatized nucleoside in the uridine case) in the low-polarity solvent required in this step.

Besides these aspects of the synthesis of SL-ATP, we also have to consider the conformation of the nitroxide group with respect to the ribose ring and the multiplicity of structural states that can be adopted by SL-ATP and its precursors. For example, we find that, as with the spiroketal acetate precursors of the spin-labeled uridine, the corresponding precursors of SL-ATP, compounds **3** and **4** (Scheme I), show NMR evidence of two predominant conformations that interconvert slowly on the NMR time scale at ambient temperature. In contrast, the reduced SL-ATP, and by implication SL-ATP **5** itself, are in rapid conformational exchange. The nitroxyl group will therefore describe an arclike motion with respect to the ribose ring. We have also had to consider to what extent SL-ATP (or SL-ADP) is rigidly bound to myosin and whether there is motion of the ribose moiety with respect to the myosin head.

We needed to develop a method to regenerate SL-ATP in situ from its diphosphate formed as a result of triphosphatase activity of the muscle because a good regenerating system would enable experiments to be done at lower free concentrations of nucleotide analog and hence overcome the problems associated with the EPR signal from unbound nucleotide interfering with the bound signal.

We first attempted to regenerate SL-ATP from SL-ADP using pyruvate kinase and creatine kinase in light of Hiratsuka's (1983) successful use of these enzymes for regenerating ribose-modified ATP. In neither case was SL-ADP a substrate of the enzymes. However, SL-ATP and SL-ADP were found to be substrates for yeast PGK. The reaction of SL-ADP and 1,3-bisphospho-D-glycerate to form SL-ATP and 3-phospho-D-glycerate catalyzed by PGK favors SL-ATP formation. Furthermore, the reaction of D-glyceraldehyde 3-phosphate, P_i, NAD^+, and SL-ADP to form NADH, 3-phosphoglycerate, and SL-ATP in the presence of GAP-DH and PGK was sufficiently energetically favorable for a continuous spectrophotometric assay of SL-ADP phosphorylation based on absorbance changes at 340 nm associated with NADH formation to be established. From the results of these assays we developed an SL-ATP regenerating system based on PGK and 1,3-bisphospho-D-glycerate. The favorable energetic coupling of reactions catalyzed by these two enzymes has been used previously in a spectrophotometric assay of P_i generated by heavy meromyosin ATPase activity (Trentham et al., 1972).

Finally, we tested SL-ATP as a substrate of myosin and actomyosin, and for its ability to support contraction and induce relaxation in permeabilized muscle fibers. We examined its EPR spectrum when bound to isolated myosin filaments, myofibrils, and muscle bundles and compared the results with those obtained with other EPR probes of muscular contraction.

EXPERIMENTAL PROCEDURES

General Procedures. Anhydrous DMF was purchased from Aldrich Chemical Co. and transferred by syringe under an atmosphere of dry nitrogen. HPLC grade acetonitrile and pyridine were dried by distillation over phosphorus pentoxide and KOH, respectively. Hexamethylphosphoric triamide was dried by distillation from calcium hydride under reduced pressure and stored over molecular sieves. 1,1'-Carbonyldiimidazole was purchased from Lancaster Synthesis and used only if the melting point was above 110 °C. TEAB buffer was prepared by bubbling CO_2 through an ice-cold aqueous solution of 1.0 M redistilled triethylamine until the pH decreased to 7.4. Yeast PGK and rabbit muscle GAP-DH were purchased from Boehringer Mannheim as crystalline suspensions in 3.2 M ammonium sulfate solution. 2',3'-*O*-(1-Oxy-2,2,6,6-tetramethylpiperidylidene)uridine (spin-labeled uridine) was synthesized as previously described (Alessi et al., 1991). All other reagents were of the highest available purity and used without further treatment.

^1H NMR spectra were obtained in D_2O–25 mM potassium phosphate, pD 7.0, at 500 MHz on a Bruker AMX spectrometer and referenced to sodium 3-(trimethylsilyl) [2,2,3,3-$^2H_4$]propionate as internal standard. ^{31}P NMR spectra were recorded at 81 MHz with broad band proton decoupling in D_2O–50 mM Tris buffer, pH 9.0, on a Bruker WM 200 spectrometer and referenced to 85% H_3PO_4 as external standard. Conventional EPR experiments were performed on a Bruker ER300 spectrometer (IBM Instruments Inc., Danbury, CT) using a TM_{110} cavity modified to accept a fiber-containing capillary parallel to the static magnetic field (Fajer et al., 1988). For fiber EPR experiments 0.3-mm fiber bundles were placed in a 0.6-mm (i.d.) glass capillary and held isometrically by a surgical thread tied at each end. Test solutions were continuously flowed over the fibers at a rate of 0.2 mL/min. The myosin filament and myofibril EPR experiments were performed using a standard TE cavity.

Sample Preparation. Rabbit myosin S1 carrying alkali light chain 1 [S1(A1)] used in the ATPase experiments was prepared according to the method of Trayer and Trayer (1988). Myosin filaments used in EPR experiments were a gift from Mr. C. L. Berger, who prepared myosin as described by Margossian and Lowey (1982). Rabbit skeletal muscle actin was prepared from muscle acetone powder (Barany et al., 1957) by the method of Spudich and Watt (1971). Glycerinated psoas muscle fibers used in the EPR experiments were prepared from New Zealand White rabbits as described by Fajer et al. (1988). Myofibrils were prepared by homogenization of glycerinated muscle fibers using a Tekmar homogenizer.

ATPase Assays. The steady-state SL-ATP and ATP hydrolysis rates were measured at 25 °C over a period of 10 min by the rate of P_i release (Fiske & Subbarrow, 1925). The assays were done using solutions (total volume 1.0 mL) of, for ammonium/EDTA ATPase, 50 mM TEA-HCl, pH 7.5, 0.5 M NH_4Cl, 10 mM EDTA, 0.005 mg S1(A1), and 4 mM TEA-ATP or SL-ATP, for calcium (high salt) ATPase, 50 mM TEA-HCl, pH 7.5, 0.6 M KCl, 10 mM $CaCl_2$, 0.0165 mg S1(A1), and 4 mM TEA-ATP or SL-ATP, and, for actin-activated MgATPase, 25 mM TEA-HCl, pH 7.5, 2.5 mM $MgCl_2$, 0.033 mg S1(A1), 2 mM TEA-ATP or SL-ATP, and F-actin varied over the range 0–50 μM.

Muscle Fiber Preparation and Physiological Measurements. Muscle fibers from the rabbit psoas muscle were dissected and permeabilized as described by Eastwood et al. (1979) and mounted in the apparatus described previously (Ferenczi et al., 1984). Muscle bundles were placed on a glass dissecting dish held at 4–8 °C and filled with silicone oil. Individual muscle fiber segments were separated from the bundle. The ends of the muscle fiber segments were crimped in aluminum T-clips as described previously (Goldman & Simmons, 1984). The muscle fibers were then transferred to an experimental stainless steel trough filled with 20 μL of relaxing solution (see legend to Figure 2) at a temperature of 20 °C. Muscle fibers were held between two stainless steel hooks attached to a tension transducer (silicon strain gauge AE801 from AME, Horten, Norway) and to the moving arm of a motor (Model 300S, Cambridge Instruments, Cambridge, MA). The solution in which the muscle fiber was bathed could be rapidly changed by moving a new trough below the fiber and raising it as described previously (Ferenczi, 1986). Muscle fiber dimensions (length between the T-clips, cross-sectional area, and sarcomere length) were determined by observation through a 40× Zeiss water immersion objective and a 25× Leitz Periplan eyepiece. Cross-sectional area was calculated by assuming an elliptical cross section of the fibers.

Maximal shortening velocity was measured by the "slack-test" method of Edman (1979) in three consecutive contractions during which the muscle length was reduced sufficiently to allow for a measurable shortening time at zero load. The amplitudes of shortening of the first and third contractions were 0.374 mm, and that of the second contraction was 0.299 mm, measured microscopically. The shortening step was achieved in less than 0.3 ms. The third contraction was identical to the first and served as a control. The time for taking up the slack was determined by a linear regression to the data collected soon after tension was clearly above baseline and calculating the intersection of the regression line with the zero force level. The value obtained for the second contraction was subtracted from the average of the values obtained for the first and third contractions. The time interval was the time taken for a shortening of 75 μm. The muscle fiber was restored to its original length after the fiber was returned to relaxing solution.

The rate of force redevelopment of synchronized cross-bridges was determined by the method of Brenner and Eisenberg (1986) in which a large decrease in muscle length is shortly followed by a rapid return to the initial length. This procedure resulted in an approximately exponential force redevelopment, for which the rate constant was calculated using the program Enzfit (Leatherbarrow et al., 1985).

Stiffness was calculated from the relationship between the force response to an imposed small-amplitude stretch of activated muscle fibers (Ford et al., 1977). Imposed length changes (≈0.2–0.5% of muscle length) were complete in 0.2 ms. The same procedure was used in the presence of ATP and in the presence of SL-ATP to obtain direct comparisons between the two substrates.

The rate of phase 4, the slow recovery phase following an imposed shortening on the muscle fiber (Huxley & Simmons, 1971), was obtained by measuring the half-time for tension recovery. The same procedure was applied for tests in ATP and SL-ATP to obtain direct comparisons between the two substrates.

Enzymic Synthesis of 1,3-Bisphospho-D-glycerate. This compound was synthesized and characterized essentially as described by Furfine and Velick (1965) and Trentham (1971). D,L-Glyceraldehyde 3-phosphate was prepared in the acid form from its diethyl ketal monobarium salt (100 mg, 264 μmol, Sigma). The solution (12 mL, 10 mM in D-glyceraldehyde 3-phosphate) was adjusted to pH 7.1 with 0.2 M phosphate, pH 8.0 (1.2 mL), and 1.0 M NaOH (0.55 mL) and treated with aliquots (0.4 mL each) of 12 mM NAD^+, 1.0 M sodium pyruvate, and 10 mM 2-mercaptoethanol. EDTA (10 mM, 1.6 mL) was added followed by $(NH_4)_2SO_4$ suspensions of rabbit muscle GAP-DH (2.4 mg of protein) and L-lactate dehydrogenase (0.2 mg of protein), incubated for 10 min at 20 °C, and cooled on ice. The aqueous solution was added to a 10-fold excess of ice-cold acetone. The precipitate that formed was collected by centrifugation at 5000 rpm (caution: fire risk through electric spark) and washed with more cold acetone. The pellet was put under a water pump vacuum to remove acetone and resuspended quantitatively in 10 mM imidazole, pH 7.5 (3 mL). Vigorous vortexing was required to break up the pellet, and the resulting solution was recentrifuged to remove precipitated protein. The supernatant containing 1,3-bisphospho-D-glycerate was adjusted to pH 7.1 with aqueous NaOH and immediately stored at −70 °C. The concentration of 1,3-bisphospho-D-glycerate was assayed by measuring the change in absorbance at 340 nm (ϵ = 6220 M^{-1} cm^{-1}) when 5 μL of the stock reagent was added to a solution (1 mL) of 0.25 mM NADH, 1 mM EDTA, 1 mM 2-mercaptoethanol, and GAP-DH (0.094 mg). A total of 3.5 mL of 21 mM 1,3-bisphospho-D-glycerate was produced (61% yield). P_i present in this preparation was 15 mM as determined by a purine nucleoside phosphorylase/2-amino-6-mercapto-7-methylpurine ribonucleoside assay (Webb, 1992).

1,3-Bisphospho-D-glycerate is unstable and was found, using the above assay, to have a half-life of 100 min and decompose to 3-phospho-D-glycerate with a first-order rate constant of 6.9×10^{-3} min^{-1} at 22 °C, pH 7.1. When stored on ice at pH 7.1, the half-life of 1,3-bisphosphoglycerate was found to be 900 min. After 2 weeks at −70 °C, the concentration of 1,3-bisphospho-D-glycerate had diminished by 15%.

Phosphoglycerate Kinase Assays. The equilibria of the coupled reactions involving the interconversion of NAD^+ and NADH and of SL-ATP and SL-ADP catalyzed by GAP-DH and PGK are such that a spectrophotometric assay is possible in either direction. The reaction of SL-ATP with 3-phospho-D-glycerate was monitored continuously at 340 nm and 25 °C using a solution (1 mL total volume) of 0.1 M TES, pH 7.0, 6.2 mM 3-phospho-D-glycerate, 0.2 mM NADH, 2.1 mM $MgCl_2$, 0.11 mM EDTA, 0.11 mM 2-mercaptoethanol, PGK (0.025 mg), and GAP-DH (0.035 mg). SL-ATP was added to start the reaction. The reaction of SL-ADP with 1,3-bisphospho-D-glycerate was assayed at 25 °C in a solution (1 mL final volume) of 0.1 M TES, pH 7.0, 1 mM NAD^+, 1 mM phosphate, 2 mM D,L-glyceraldehyde 3-phosphate, 2.1 mM $MgCl_2$, 0.11 mM EDTA, 0.11 mM 2-mercaptoethanol, PGK (0.035 mg), and GAP-DH (0.035 mg). SL-ADP was added to start the reaction. The reactions of SL-ATP and SL-ADP with PGK were monitored at 12 different concentrations of nucleotide over the range 0–1.5 mM.

1,3-Bisphospho-D-glycerate/3-Phospho-D-glycerate Kinase Regenerating System. A suspension of yeast PGK (1 mL of 10 mg/mL in 3.2 M ammonium sulfate) was dialyzed overnight against 50 mM imidazole hydrochloride, pH 7.1 (5 L), without any loss in enzymic activity. In the regenerating system used for muscle fiber experiments the final concentration of dialyzed phosphoglycerate kinase was 0.25 mg/mL, and that of 1,3-biphospho-D-glycerate was 2 mM.

2′,3′-O-(1-Acetoxy-2,2,6,6-tetramethyl-4-piperidylidene)-adenosine 5′-Monophosphate (*Scheme I*, **3**). The free acid form of AMP monohydrate (2.2 g, 6 mmol) was suspended in dry DMF (50 mL), and the solvent was removed under vacuum (<1 mmHg) at a bath temperature of 35 °C. The procedure was repeated a further three times to remove traces of water from the nucleotide, and at the end of the final cycle the residue was thoroughly pumped under vacuum to ensure complete removal of the DMF.

In a separate flask, toluenesulfonic acid monohydrate (5.7 g, 30 mmol) was similarly dried by repeated vacuum evaporation from anhydrous acetonitrile (4 × 50 mL) and then dissolved in anhydrous acetonitrile (440 mL) together with 1-acetoxy-4-methoxy-2,2,6,6-tetramethyl-1,2,5,6-tetrahydropyridine (20 g, 88 mmol) prepared by the method of Alessi et al. (1991). This solution was added rapidly to the dried nucleotide, and the resulting suspension was stirred in a sealed flask at room temperature. After 7 days, the undissolved fraction of AMP was removed by filtration, the filtrate was added to 10 mM TEAB buffer, pH 7.4 (3 L), and the mixture was extracted with petroleum ether (3 × 500 mL). The organic extracts were discarded, and the aqueous solution was adjusted to pH 7.4 and applied to a DEAE-cellulose column (500 mL bed volume, pre-equilibrated with 10 mM TEAB, pH 7.4, at a flow rate of 80 mL/h). After loading, the column was washed with 10 mM TEAB, pH 7.4, until the absorbance (260 nm) of the effluent returned to zero and then eluted with a linear gradient formed from 10 and 250 mM TEAB, pH 7.4 (each 1.5 L). Fractions were collected and monitored by UV and analytical HPLC (Merck Lichrocart C8 column, 25 cm × 4.6 mm; mobile phase 45% MeOH in 10 mM sodium acetate, pH 6.5; flow rate 1.5 mL/min). Only AMP, toluenesulfonic acid, and the required product bound to the DEAE-cellulose column, and these had HPLC retention times of 1.5, 1.6, and 3.3 min, respectively. All fractions containing the spiroketal were pooled and concentrated under reduced pressure and then evaporated under vacuum with methanol several times to remove buffer salts. The product at this stage contained about 40% unreacted AMP and was further purified in 100-μmol batches by isocratic reversed-phase preparative HPLC (Waters C18, 25 cm × 22 mm; mobile phase 35% methanol in 10 mM sodium acetate, pH 6.5; flow rate 4 mL/min). Fractions were collected and assayed by analytical HPLC (see above); those containing the pure spiroketal **3** were combined and concentrated under reduced pressure to remove most of the methanol and desalted on a DEAE-cellulose column as described above, and the eluted material was freed from buffer salts as before to give the pure spiroketal **3** as its triethylammonium salt (1.2 mmol; 20% yield). For NMR analysis a sample of the triethylammonium spiroketal was converted to the sodium salt by passing an aqueous solution of the spiroketal in water (1 mL, 1 mM) down a Dowex 50W column (Na^+ form, 2 mL). A set of single-frequency decoupling ^1H NMR experiments was performed to assign resonances to conformer A or B.

^1H NMR δ 8.60 (s, 0.5 H, purine H), 8.55 (s, 0.5 H, purine H), 8.23 (s, 0.5 H, purine H), 8.21 (s, 0.5 H, purine H), 6.34 (d, 0.5 H, $J_{1',2'}$ = 2.9 Hz, H-1′$_A$), 6.23 (d, 0.5 H, $J_{1',2'}$ = 3.7 Hz, H-1′$_B$), 5.48 (d/d, 0.5 H, $J_{2',3'}$ = 5.9 Hz, H-2′$_A$), 5.32 (d/d, 0.5 H, $J_{2',3'}$ = 5.9 Hz, H-2′$_B$), 5.22 (br d, 0.5 H, H-3′$_B$), 5.15 (d/d, 0.5 H, $J_{3',4'}$ = 2.2 Hz, H-3′$_A$), 4.78 (br s, 0.5 H, H-4′$_B$), 4.58 (m, 0.5 H, H-4′$_A$), 3.9–4.05 (m, 2 H, H-5′), 2.04–2.26 (m, 3 H, H3″ and H5″), 2.20 and 2.16 (2 × s, 2

× 1.5 H, CH_3CO), 1.84 and 1.81 (2 × d, 2 × 0.5 H, J_{gem} = 11.5 Hz, 2 × 0.5 of H-3″ or 5″), 1.41 (s, 1.5 H, 0.5 CH_3), 1.36 (s, 1.5 H, 0.5 CH_3), 1.33 (s, 1.5 H, 0.5 CH_3), 1.26 (s, 1.5 H, 0.5 CH_3), 1.12 (s, 1.5 H, 0.5 CH_3), 1.11 (s, 1.5 H, 0.5 CH_3), 1.06 (s, 1.5 H, 0.5 CH_3), 1.04 (s, 1.5 H, 0.5 CH_3); ^{31}P NMR δ 4.66 and 4.64 (2 × s).

2′,3′-O-(1-Acetoxy-2,2,6,6-tetramethyl-4-piperidylidene)-adenosine 5′-Triphosphate (Scheme I, **4**). The AMP spiroketal acetate was pyrophosphorylated using modifications of the procedures of Hoard and Ott (1965) and Maeda et al. (1977). Trioctylamine (600 μmol, 263 μL) was added to a solution of **3** (600 μmol) as its triethylammonium salt in anhydrous pyridine (25 mL), which was then concentrated to dryness by rotary evaporation under vacuum (<1 mmHg) at 35 °C. The residue was dissolved in anhydrous DMF (20 mL), which was removed by vacuum evaporation, and this cycle was repeated two more times. The residue was then dissolved in anhydrous DMF (1 mL), 1,1′-carbonyldiimidazole (195 mg, 1.2 mmol) was quickly added, and the resulting solution was left at room temperature in a sealed flask for 5 h. Methanol (60 μL, 1.73 mmol) was then added, and after a further 30 min, the solvent was removed by rotary evaporation. The trioctylammonium salt of pyrophosphate (16.8 mmol), prepared as described by Hoard and Ott (1965) using trioctylamine instead of tributylamine, was dissolved in anhydrous hexamethylphosphoric triamide (30 mL). This solution was then rapidly added to the activated AMP spiroketal acetate, and the resulting mixture was vigorously stirred in a sealed flask. After 48 h, the reaction mixture was added to 10 mM TEAB, pH 7.4 (1 L), and the resulting cloudy solution was adjusted to pH 7.4, applied to a DEAE-cellulose column (bed volume 250 mL) as previously described, and eluted with a linear gradient formed from 10 and 350 mM TEAB, pH 7.4 (each 2 L), at a flow rate of 70 mL/h. Fractions were analyzed by reversed-phase HPLC (conditions as above), and the retention time for the ATP spiroketal acetate **4** was 1.8 min, which corresponded to the largest peak on the DEAE-cellulose column (eluting at 300 mM TEAB). Fractions containing pure product were combined and freed from buffer salts as above to afford the ATP spiroketal **4** as its triethylammonium salt (410 μmol; 68%). A sample of **4** was converted to the sodium salt and analyzed by ^1H NMR as described above: ^1H NMR δ 8.45 (s, 0.5 H, purine H), 8.43 (s, 0.5 H, purine H), 8.21 (s, 1 H, purine H), 6.31 (d, 0.5 H, $J_{1',2'}$ = 2.5 Hz, H-1′$_A$), 6.23 (d, 0.5 H, $J_{1',2'}$ = 3.1 Hz, H-1′$_B$), 5.41 (d/d, 0.5 H, $J_{2',3'}$ = 5.9 Hz, H-2′$_A$), 5.27 (m, 2 × 0.5 H, H-2′$_B$, H-3′$_B$), 5.17 (d/d, 0.5 H, $J_{3',4'}$ = 2.2 Hz, H-3′$_A$), 4.83 (m, 0.5 H, H-4′$_B$, under HDO peak), 4.63 (br s, 0.5 H, H-4′$_A$), 4.1–4.3 (m, 2 H, H-5′), 2.26–2.04 (m, 3 H, H3″ and H5″), 2.21 and 2.17 (2 × s, 2 × 1.5 H, CH_3CO), 1.85 and 1.82 (2 × d, 2 × 0.5 H, J_{gem} = 12.0 Hz, 2 × 0.5 H of H-3″ or -5″), 1.41 (s, 1.5 H, 0.5 CH_3), 1.36 (s, 1.5 H, 0.5CH_3), 1.35 (s, 1.5 H, 0.5CH_3), 1.25 (s, 1.5 H, 0.5CH_3), 1.14 (s, 1.5 H, 0.5CH_3), 1.13 (s, 1.5 H, 0.5CH_3), 1.07 (s, 1.5 H, 0.5CH_3), 1.05 (s, 1.5 H, 0.5CH_3); ^{31}P NMR δ –5.02 and –5.07 (2 × d, $J_{\beta,\gamma}$ = 20.8 Hz, γ-P), –10.46 and –10.58 (2 × d, $J_{\alpha,\beta}$ = 19.5 Hz, α-P), –20.17 and –21.09 (2 × t, β-P).

2′,3′-O-(1-Oxy-2,2,6,6-tetramethyl-4-piperidylidene)adenosine 5′-Triphosphate (SL-ATP, Scheme I, **5**). The ATP spiroketal acetate **4** (400 μmol) in 50% aqueous methanol (62 mL) was added to a solution of KOH (1.34 g) in methanol (21 mL), and the mixture was left at room temperature and open to the atmosphere. The reaction was monitored by HPLC (Merck Lichrocart C8; mobile phase 12% acetonitrile in 50 mM KH_2PO_4, pH 5.5; flow rate 1.5 mL/min). Retention times for the spiroketal acetate and SL-ATP were 4.0 and 13.0 min, respectively. When the hydrolysis/oxidation reaction was complete (60 h), the reaction mixture was neutralized with 1 M HCl (24 mL) and diluted with 10 mM TEAB, pH 7.4 (600 mL). The solution was applied to a DEAE-cellulose column (bed volume 200 mL) at a flow rate of 75 mL/h. The column was eluted with a linear gradient formed from 10 and 350 mM TEAB (each 2 L), and fractions were analyzed by analytical HPLC as above. Fractions containing the product were seen to contain an impurity (approximately 3%, HPLC retention time of 1.2 min) which was identified as free ATP. These fractions were combined and freed from buffer salts as above. The contaminated spin-labeled product (100-μmol batches) was purified by preparative HPLC (Waters C18; mobile phase 5% acetonitrile in 10 mM sodium acetate, pH 6.5; flow rate 4 mL/min). Fractions containing pure spin label (total 360 μmol) were pooled, desalted on DEAE-cellulose as described above, and stored at –70 °C either as the triethylammonium salt or after treatment with Dowex 50W (Na^+ form) as the sodium salt.

^1H NMR δ 8.50 (br s, purine H), 8.25 (br s, purine H), 6.47 (very br s, H1′) 5.75 (very br s, H-2′ and H-3′), 4.8 (H-4′ under HDO peak), 4.22 (very br s, H-5′), none of the protons on the piperidine ring was observable; ^{31}P NMR δ –5.09 (d, $J_{\beta,\gamma}$ = 20.8 Hz, γ-P), –10.48 (d, $J_{\alpha,\beta}$ = 18.3 Hz, α-P), –21.04 (t, β-P).

The EPR spectrum recorded at 9.81 GHz (25 mM potassium phosphate, pH 7.5) showed a triplet centered at 3470.58 G, with a hyperfine splitting of 16.8 G.

2′,3′-O-(1-Hydroxy-2,2,6,6-tetramethyl-4-piperidylidene)-adenosine 5′-Triphosphate (Reduced SL-ATP). A portion of SL-ATP (sodium salt, 1 mM, 500 μL, 25 mM potassium phosphate, pD 7.0) was reduced to the diamagnetic *N*-hydroxy spiroketal derivative of SL-ATP by the addition of ascorbic acid (0.1 M in D_2O adjusted to pD 7.0, 3 μL added) to enable a complete NMR characterization of SL-ATP.

^1H NMR of reduced SL-ATP δ 8.42 (s, 1 H, purine H), 8.21 (s, 1 H, purine H), 6.26 (br s, 1 H, $J_{1',2'}$ not resolved, H-1′), 5.37 (br s, 1 H, H-2′), 5.22 (m, 1 H, H-3′), 4.71 (br s, 1 H, H-4′), 4.13–4.28 (m, 2 H, H-5′), 2.19 (s, 2 H, H-3″ and H-5″), 2.08–1.90 (br m, 2 H, H-3″ and H-5″), 1.37 (s, 3 H, CH_3), 1.35 (s, 3 H, CH_3), 1.32 (s, 3 H, CH_3), and 1.28 (s, 3 H, CH_3); ^{31}P NMR δ –5.07 (d, $J_{\beta,\gamma}$ = 19.5 Hz, γ-P), –10.5 (d, $J_{\alpha,\beta}$ = 18.3 Hz, α-P), –21.02 (t, β-P).

2′,3′-O-(1-Oxy-2,2,6,6-tetramethyl-4-piperidylidene)adenosine 5′-Diphosphate (SL-ADP). SL-ATP was dephosphorylated enzymatically to SL-ADP by S1(A1), in a solution (6 mL total volume) of 10 mM TEA-HCl, pH 7.5, 5 mM SL-ATP, 5 mM $MgCl_2$, and 18 mg of S1(A1) (1.0 mL dialyzed into 25 mM TEA-HCl, pH 7.5). The reaction was monitored by analytical anion-exchange HPLC [Anachem Spherisorb S5SAX-2611 column, 25 cm × 4.6 mm; mobile phase 20% MeOH in 50 mM $(NH_4)_2HPO_4$ adjusted to pH to 5.9 with 10 M HCl before addition of methanol; flow rate 1.5 mL/min]. SL-ATP and SL-ADP were found to have retention times of 17.1 and 11.8 min, respectively. The reaction was complete within 30 min, after which time ethanol (10 mL) was added to precipitate S1(A1), and the resulting mixture was centrifuged at 30000 rpm for 10 min. The supernatant was then added to 10 mM TEAB, pH 7.4 (160 mL), as above, and applied to a DEAE-cellulose column (bed volume 50 mL; flow rate 40 mL/h). SL-ADP was eluted with a linear gradient formed from 10 and 300 mM TEAB, pH 7.4 (300 mL each), and fractions containing the spin-labeled nucleotide were pooled, evaporated under reduced pressure, and converted to

the sodium salt was described above.

RESULTS

Synthesis of SL-ATP. In our previous paper (Alessi et al., 1991) we showed that the acid-catalyzed condensation of the enol ether **1** with the 2′,3′-diol system of uridine could not be performed in dipolar aprotic solvents such as DMF or dimethyl sulfoxide. However, in the case of nucleotides, solvents such as these would be required to dissolve the nucleotide reagent. In preliminary experiments to promote the solubility of an adenine nucleotide in a solvent of low polarity (tetrahydrofuran or dioxane) compatible with the desired reaction, we examined various AMP and ATP derivatives including N^6-benzoyl-AMP (Hampton & Slotin, 1975), its 1-(2-nitrophenyl)ethyl ester, and the corresponding P^3 ester of ATP (Walker et al., 1988). The first and last compounds were not usefully soluble in tetrahydrofuran, dioxane, or acetonitrile, but N^6-benzoyl-AMP 1-(2-nitrophenyl)ethyl ester was freely soluble in these solvents. However, it became clear (data not shown) that the rate of reaction with the enol ether **1** to produce the required spiroketal was comparable with the rate of acid-catalyzed depurination and that the latter reaction occurred even more rapidly in the spiroketal product. N^6-Acylation is known to promote the depurination reaction (Froehler & Matteucci, 1983), and these attempts were abandoned. In the course of many trial experiments we found that the presence of a 5-fold excess of toluenesulfonic acid promoted the solubility of AMP to a limited extent in acetonitrile and thereby allowed the desired reaction to proceed. The route used to synthesize the spin-label ATP analog, in which the free radical piperidine nitroxide is rigidly attached as a spiroketal to the 2′ and 3′ ribose hydroxyl groups of ATP, is shown in Scheme I. The key role of the enol ether (**1**) in the condensation reaction with the mononucleotide has been emphasized in our earlier work (Alessi et al., 1991).

Characterization of the spiroketal structures rests primarily on the similarity of NMR spectral features with those of the uridine spiroketals prepared recently (Alessi et al., 1991). The ^{1}H NMR spectrum of SL-ATP is naturally very broad, and none of the protons of the piperidine ring is observable. Reduction of **5** with 0.6 equiv of ascorbate yields the hydroxylamine derivative, and the ^{1}H NMR spectrum of the methyl region of this compound, compared with that of **4**, is shown in Figure 1. Care must be taken in the reduction reaction as more powerful reducing agents (e.g., sodium dithionite) can overreduce the nitroxide to the amine with a concomitant downfield shift of the methyl signals (data not shown). The ^{1}H NMR signals of the *N*-acetoxy spiroketal intermediates **3** and **4** appeared as pairs of signals of about equal intensity (see Figure 1a, for the spectrum of the *gem*-dimethyl groups of the piperidine ring of **4**). We have previously ascribed this phenomenon to the presence of two slowly interconverting conformations of the piperidine ring (Alessi et al., 1991). Removal of the acetoxy protecting group allows these conformers to exchange more rapidly (Figure 1b) and only a single set of signals for each methyl group is seen, in accord with the temperature dependence study of the exchange rates reported earlier (Alessi et al., 1991).

The ^{31}P NMR spectra showed broadly similar effects to those observed in the ^{1}H spectra. In particular, the three phosphate groups in the *N*-acetoxy triphosphate **4** appeared as pairs of signals reflecting the two conformations present in the compound. The pairs of signals show differing degrees of relative chemical shift (see Experimental Procedures), presumably because of the different spatial relationships

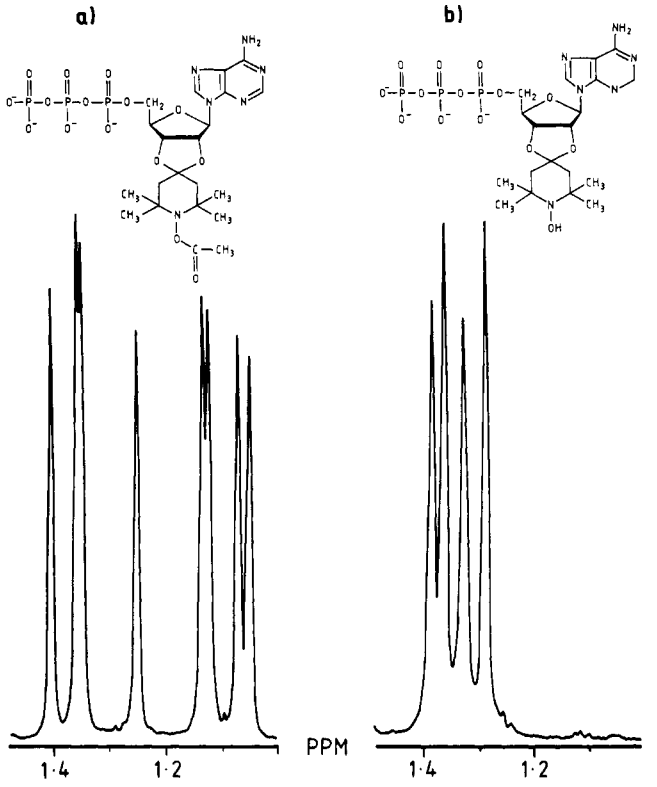

FIGURE 1: ^{1}H NMR spectra of the geminal methyl region of (a) 2′,3′-*O*-(1-acetoxy-2,2,6,6-tetramethyl-4-piperidylidene)adenosine 5′-triphosphate (**4**) and (b) 2′,3′-*O*-(1-hydroxy-2,2,6,6-tetramethyl-4-piperidylidene)adenosine 5′-triphosphate.

Table I: Rates of Hydrolysis of SL-ATP and ATP by S1(A1)

ATPase activity[a]	nucleotide substrate	rate [μmol (mg of S1(A1))$^{-1}$ min^{-1}]
NH_4^+/EDTA	ATP	4.1
	SL-ATP	2.2
Ca^{2+}/high salt	ATP	1.9
	SL-ATP	1.4

[a] The methods for measurement of the ATPase activities are given under Experimental Procedures

between the three phosphates and the anisotropic acetoxy group. When the spectra of SL-ATP and its reduced diamagnetic derivative are compared, there is a clear trend in the line widths of the phosphate signals. In the reduced derivative, all of these phosphate signals have line widths in the range 5.2–7.0 Hz, but in SL-ATP the line widths are 11.75, 10.7, and 7.1 Hz for the α, β, and γ phosphate groups, respectively. This differential line broadening is compatible with the increasing distance of the phosphorus atoms from the paramagnetic center.

SL-ATP as a Substrate for S1. Tables I and II compare the activities of SL-ATP and ATP as substrates for S1(A1). In the absence of actin, rates for the ammonium/EDTA- and high-salt Ca-ATPase activities were 53 and 73%, respectively, of those obtained with ATP (Table I). In the presence of actin, the V_{max} value of the S1–MgATPase was 50% greater using SL-ATP as a substrate instead of ATP, corresponding to turnover rates of 18.2 and 12.3 s^{-1}, respectively. The apparent K_m for actin was also slightly higher with SL-ATP (Table II). The kinetic values found for rabbit S1(A1) with ATP are similar to those reported earlier under similar conditions (Wagner et al., 1979).

Table II: Kinetic Parameters of the Actin-Activated MgATPase of S1(A1)[a]

nucleotide substrate	K_m actin[b] (μM)	V_{max}[b] [μmol (mg of S1(A1))$^{-1}$ min^{-1}]
ATP	33	6.4
SL-ATP	42	9.5

[a] The methods for determination of the ATPase activities are given under Experimental Procedures. [b] The kinetic parameters were obtained from a plot of [nucleotide]/initial rate vs [nucleotide] (Hanes, 1932). Initial rates of the S1(A1) MgATPase in the absence of actin were subtracted from the actin-activated rates. These were the same with both ATP and SL-ATP as substrates, in the range 0.015–0.020 μmol (mg of S1(A1))$^{-1}$ min^{-1}.

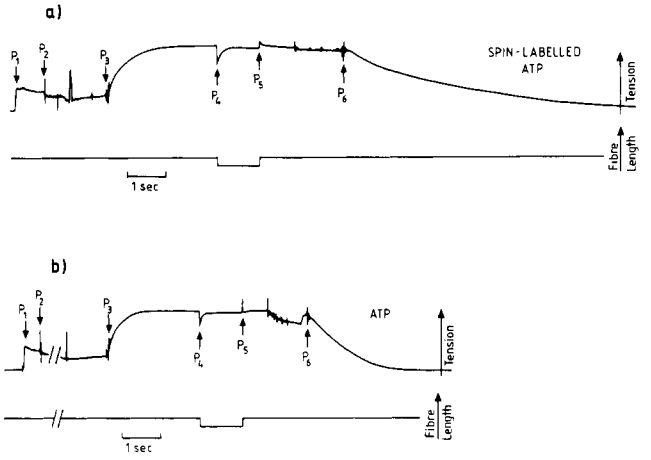

FIGURE 2: Tension measurements on a single permeabilized fiber from rabbit psoas muscle in the presence of SL-ATP (a) followed by ATP (b). At the outset, the fiber (total length between T-clips of 1600 μm, cross-sectional area of 4.79×10^{-9} m^2, and a sarcomere length of 2.38 μm) was relaxed in a solution containing MgATP (5 mM), Mg^{2+} (2 mM), EGTA (30 mM), and TES (60 mM) at pH 7.1 and 20 °C. The ionic strength of all solutions was kept at 0.15 M by calculating the appropriate amount of potassium propionate to be added. At the various time points indicated, the fiber was transferred between solutions that differed only in the ingredients indicated below: At P1, the rigor state was induced by incubation in a solution devoid of nucleotide and with 10 mM EDTA to chelate and remove Mg^{2+}. At P2, the fiber was transferred to a solution containing no nucleotide but 2 mM Mg^{2+} and 0.032 mM Ca^{2+} (Ca^{2+}-rigor). At P3, the fiber was transferred to a solution similar to Ca^{2+}-rigor to which 4 mM nucleotide had been added. This activating solution caused the rise in isometric tension to a plateau of 170.9 kN/m^2 above the relaxed level (before P1) in (a) and of 150.0 kN/m^2 in (b). At P4, the muscle length was decreased in both cases by 10.94 μm, corresponding to an overall length change of 0.68%. This change in muscle length was accompanied by an instantaneous fall in force. Force then recovered, nearly to the value before the applied length change. At P5, the muscle length was returned to its initial value by applying a rapid stretch. A fast tension rise accompanies the length change, and a rapid return to the initial tension level follows. At P6, calcium was removed by immersing the fiber in a solution containing 30 mM EGTA, with no calcium (relaxing solution). This causes relaxation of the fiber.

SL-ATP as a Substrate for Muscle Contraction. Comparison of the effects of ATP and SL-ATP on the tension and stiffness measurements on single-skinned rabbit psoas muscle fibers is shown in Figure 2. At the various time points indicated the fibers were transferred between different solutions. At the start, the fibers were relaxed in Mg–nucleotide. The rate of tension development and the level of isometric tension produced by the fibers (after P_3) were about the same whether MgATP or MgSL-ATP was used as the substrate. Stiffness measurements on the fibers were made by estimating the force response to an imposed small-amplitude length change (at P_4), and it was found that the stiffness of the fibers activated with SL-ATP was about the same as for fibers activated with ATP. Following the imposed shortening of the muscle fibers the rate of phase 4, the slow recovery phase (Huxley & Simmons, 1971), of the SL-ATP-activated fiber was about 60% of that by ATP. In the absence of Ca^{2+}, SL-ATP was found to relax the fibers from peak isometric tension (after P_6) about 2–3 times slower than ATP. This slower relaxation may reflect the slower off-rate of SL-ADP from myosin compared to ADP. Stiffness measurements on fibers relaxed with both nucleotides were, however, identical, confirming that SL-ATP was able fully to relax the fiber.

Further physiological tests were also made of the ability of the SL-ATP to support muscle contraction. Measurements of the maximum unloaded shortening velocity of single-skinned fibers (the slack test) were 1.6 muscle lengths s^{-1} for fibers activated with 4 mM MgSL-ATP and 4.0 muscle lengths s^{-1} for those activated with 4 mM MgATP. The rate of force redevelopment after a large decrease in muscle length shortly followed by a rapid return to the initial length (synchronizing the cross-bridges) was 1.2 s^{-1} for SL-ATP-activated fibers and 2.5 s^{-1} for ATP-activated fibers.

In these mechanical tests, the same fiber was used with both ATP and SL-ATP and the experiments were repeated several times with different fibers.

These data and those in the previous section demonstrate that SL-ATP is a good analog of ATP for the myosin ATPase activity in solution and for supporting contractile activity in muscle fibers.

Development of an ATP Regenerating System for SL-ATP Using Yeast 3-Phospho-D-glycerate Kinase. SL-ATP was found not to be a substrate for the most commonly used ATP regenerating systems employing either creatine kinase or pyruvate kinase. It was, however, found that SL-ATP and SL-ADP were substrates for yeast PGK. This was established spectrophotometrically using a coupled assay in both directions with GAP-DH. That this is achievable may be seen from consideration of the free energy changes of the coupled reactions (Lehninger, 1979; Krietsch & Bücher, 1970) and the reactant concentrations

D-glyceraldehyde 3-phosphate + P_i + NAD^+ ⇄ 1,3-bisphospho-D-glycerate + NADH

$\Delta G^{\circ\prime}$ = +6.28 kJ/mol at 20 °C, pH 7.1

SL-ADP + 1,3-bisphospho-D-glycerate ⇄ SL-ATP + 3-phospho-D-glycerate

$\Delta G^{\circ\prime}$ = −18.84 kJ/mol at 20 °C, pH 7.0

assuming that $\Delta G^{\circ\prime}$ for the kinase reaction is the same with SL-ADP and ADP as substrates. From the relationship $\Delta G' = \Delta G^{\circ\prime} + RT \ln (\prod[\text{products}]/\prod[\text{substrates}])$, it is then possible to calculate equilibrium concentrations of substrates and products preliminary to using either the generation or removal of NADH as a spectrophotometric probe for analyzing the kinetics of PGK with SL-ADP or SL-ATP, respectively, as substrate. For example, suppose a solution which initially contained 1.56 mM each of D-glyceraldehyde 3-phosphate, P_i, NAD^+, and SL-ADP was incubated with GAP-DH. At equilibrium when $\Delta G' = 0$, 0.017 mM NADH would be formed. If now PGK was added, the NADH concentration would increase to 0.56 mM with the overall concentration of the four substrates dropping from 1.56 to 1.00 mM. Similar considerations show that NADH would be removed when the two enzymes are added to solutions containing SL-ATP, 3-

Table III: PGK-Catalyzed Reaction[a] Used To Recycle SL-ADP to SL-ATP

SL-ADP + 1,3-bisphospho-D-glycerate ⇌ SL-ATP + 3-phospho-D-glycerate

nucleotide substrate	K_m[b] (μM)	V_{max}[b] [μmol (mg of PGK)$^{-1}$ min^{-1}]
SL-ADP	1.80	6.0
SL-ATP	0.90	1.9
ADP[c]	0.20	2200
ATP[c]	0.11	760

[a] The measurements of the forward and backward reactions of PGK are given under Experimental Procedures. [b] The kinetic parameters were obtained from a plot of [nucleotide]/initial rate vs [nucleotide] (Hanes, 1932). [c] From Krietsch and Bucher (1970).

phospho-D-glycerate, and NADH. The K_m and V_{max} values associated with the PGK reaction with SL-ADP and SL-ATP as substrates are shown in Table III.

Since the V_{max} values for PGK were 400-fold less for SL-ADP and SL-ATP as compared to those for ADP and ATP, it was important to check that the observed SL-ADP and SL-ATP activities were not due to the presence of ADP and ATP. This was done by carrying out assays in which the concentration of NADH generated or removed was comparable with the initial SL-ADP or SL-ATP concentration. In the presence of 0.15 mM SL-ATP, 0.31 mM NADH, 6.2 mM 3-phospho-D-glycerate, and the two enzymes, oxidation of 0.138 mM NADH occurred. Likewise, in the presence of 0.3 mM SL-ADP, 1 mM NAD^+, D-glyceraldehyde 3-phosphate, P_i, and the two enzymes, 0.27 mM NADH was formed. Thus, in either direction the change in NADH concentration must have been associated with SL-ADP or SL-ATP concentration since contaminating ADP and ATP was <1% for both nucleotides (determined by HPLC).

Testing the 1,3-Bisphospho-D-glycerate/PGK/SL-ATP Regenerating System in Muscle Fibers. Our aim was to develop an enzyme-based regenerating system which would enable SL-ADP formed by the ATPase activity of the muscle fiber to be converted back to SL-ATP. Such a backup system would in principle allow EPR studies to be made of MgSL-ATP relaxed and isometrically contracting muscle bundles, using SL-ATP concentrations of ≤100 μM. With these low concentrations of nucleotide the myosin-bound spin-labeled nucleotide signal can be anticipated to be readily seen against the larger free unbound signal. When muscle fibers were treated with these low concentrations of MgSL-ATP in the absence of a backup system, the fiber rapidly hydrolyzed the spin-labeled nucleotide to SL-ADP and went into rigor. The fact that PGK catalyzes the transfer of phosphate from 1,3-bisphospho-D-glycerate to SL-ADP enabled us to construct an SL-ATP regenerating system for use in muscle fibers in which 2 mM 1,3-bisphospho-D-glycerate and 0.25 mg/mL PGK was included in the fiber incubation mixtures.

We first tested this regenerating system with MgATP using single permeabilized rabbit psoas muscle fibers. When muscle fibers in rigor were treated with 50 μM MgATP, with and without calcium, and in the absence of a regenerating system, the fibers were found not to contract or relax. In the presence of the 1,3-bisphospho-D-glycerate/PGK regenerating system fibers could be activated from rigor with 50 μM MgATP and could be fully relaxed from peak isometric tension. This indicates that for ATP at least the regenerating system works well.

The rate of force recovery after a rapid release and restretch was compared for a fiber contracting at 5 mM MgSL-ATP with and without the PGK/1,3-bisphospho-D-glycerate regenerating system. It was found that the recovery of tension followed approximately exponential time courses with rate constants of 11 s^{-1} with the backup system and 8 s^{-1} without the regenerating system. For fibers contracting with 5 mM MgATP, the rate constant was 17 s^{-1}.

Treatment of single muscle fibers in rigor with concentrations of <1 mM MgSL-ATP in the presence and absence of calcium without the regenerating system resulted in no contraction or relaxation. On the other hand, if these fibers in rigor were treated with ≥250 μM MgSL-ATP in the presence of calcium and the PGK/1,3-bisphospho-D-glycerate regenerating system, the fibers contracted and could be relaxed from peak isometric tension by removal of calcium. Stiffness measurements made on fibers relaxed in this way showed that they were fully relaxed.

Fibers in rigor (containing Ca^{2+}) could also be induced to contract with concentrations of SL-ATP as low as 50 μM, using the PGK/1,3-bisphospho-D-glycerate regenerating system, but these activated fibers could not be relaxed from peak isometric tension with concentrations of 50 and 100 μM MgSL-ATP and required concentrations of at least 250 μM MgSL-ATP for full relaxation. If the same fibers in rigor (containing EGTA and no Ca^{2+}) were treated with 50–100 μM MgSL-ATP in the presence of the backup system, then these fibers could be relaxed fully, as confirmed by stiffness measurements. The rate for this relaxation from rigor was about 5 times slower than that observed when the fibers were relaxed with MgATP under otherwise identical conditions. It is, therefore, probable that during isometric contraction with concentrations of 50–100 μM MgSL-ATP the ATPase activity of the fiber is greater than the rate at which the regenerating system can convert MgSL-ADP back to MgSL-ATP to relax the fiber. When the fiber is relaxed from rigor with 50–100 μM MgSL-ATP in the absence of Ca^{2+}, the regenerating system, together with diffusion of SL-ATP into the fiber from the bathing medium, is able to compete favorably with the much lower ATPase activity of a muscle fiber under these conditions, thereby maintaining at high enough concentration of MgSL-ATP to enable the fiber to relax. One possibility to induce relaxation of isometrically contracting fibers using <250 μM MgSL-ATP may be to use a higher concentration of PGK in the regenerating system, but this was not explored.

These results show that using the PGK/1,3-bisphospho-D-glycerate regenerating system it is possible to get single muscle fibers to relax and contract at a much lower MgSL-ATP concentration than would otherwise be possible. This will provide the basis for future EPR work with SL-ATP.

EPR Studies with SL-ADP in Muscle Fiber Bundles and Myofibrils. The orientation of MgSL-ADP bound to rigor cross-bridges in bundles of rabbit psoas muscle fibers was investigated by carrying out EPR experiments on fiber bundles orientated both parallel (Figure 3, top) and perpendicular (Figure 3, bottom) to the magnetic field. The fiber bundles were continuously perfused in a loop system at a flow rate of 0.2 mL min^{-1}. The EPR spectra did not change if the flow rate was either stopped or doubled. In Figure 3, the original spectra are shown on the left, and on the right these spectra have been corrected by subtracting the spectrum of free SL-ADP. This correction is not perfect, because the spectrum of free label in the fiber lattice has slightly greater line widths than that of the free label in buffer, probably due to a slightly higher effective microviscosity in the fiber. The spectrum of

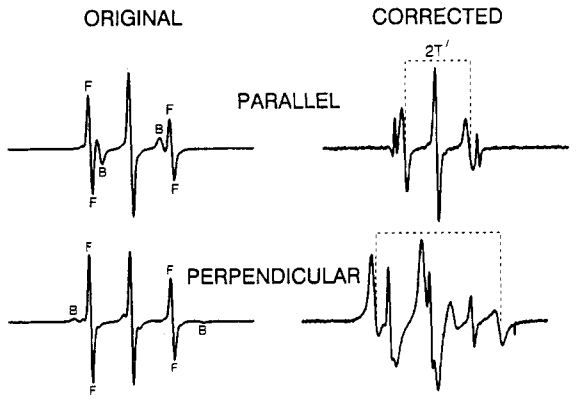

FIGURE 3: Comparison of the EPR spectra of muscle fiber bundles aligned parallel (top) and perpendicular (bottom) to the static magnetic field. The fibers were continuously perfused in a loop system with a solution of 20 mM 3-*N*-(morpholino)propanesulfonic acid–NaOH, pH 7.0, containing 130 mM potassium propionate, 2 mM EGTA, 2 mM $MgCl_2$, 1 mM NaN_3, and 50 μM SL-ADP. The signals from the unbound free SL-ADP, which gives rise to three narrow lines that dominate the original spectra (left), have been subtracted to produce the corrected spectra (right). In the original spectra (left), features of the outer spectral lines that are due to free and bound SL-ADP are designated F and B, respectively. In muscle fiber bundles oriented parallel (top right) and perpendicular (bottom right) to the magnetic field, the outer hyperfine splitting ($2T'$) values for the bound components are 26.15 and 53.4 G, respectively.

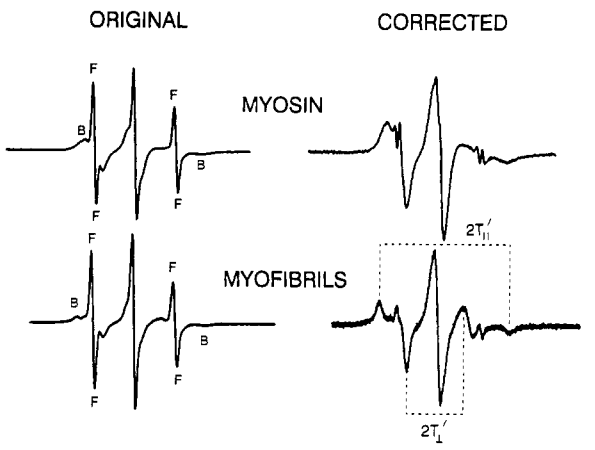

FIGURE 4: EPR spectra of SL-ADP bound to myosin filaments (top) and myofibrils (bottom). Myosin filaments (35 mg of protein/mL) and myofibrils (200 mg/mL) were suspended in 20 mM EPPS buffer, pH 8.0, containing 135 mM potassium acetate, 200 μM $MgCl_2$, and 50 μM SL-ADP. The signals from the unbound free SL-ADP, which gives rise to three narrow lines that dominate the original spectra (left), have been subtracted to produce the corrected spectra (right). In the original spectra (left), features of the outer spectral lines that are due to free and bound SL-ADP are designated F and B, respectively. The effective hyperfine tensor values for SL-ADP bound to myofibrils, used in the calculation of spin label wobble (eqs 1 and 2) and orientation (eq 3), are shown ($2T_{\parallel}'$ = 52.7 G; $2T_{\perp}'$ = 22.2 G).

MgSL-ADP bound to the myosin heads in fiber bundles oriented parallel to the magnetic field (Figure 3, top right) is narrow and the lines are sharp. The hyperfine splitting was found to be 26.15 G. This splitting is even smaller than that found for the spectrum of free SL-ADP (31.6 G), implying that the mean orientation of the spin label's principal axis relative to the fiber axis is substantially greater than 54.7°. The narrow line widths arise from a small orientational distribution and/or nanosecond rotational motion within this distribution, both of which are probably operational here. On the other hand, the EPR spectrum of MgSL-ADP bound to rigor cross-bridges oriented perpendicular to the magnetic field (Figure 3, bottom right) has a much wider hyperfine splitting, 53.4 G. The large difference between the parallel and perpendicular spectra implies that MgSL-ADP bound to the rigor cross-bridges has a narrow orientational distribution relative to the fiber axis.

Control experiments showed that the bound MgSL-ADP signal arising from the fiber bundles was not affected by including either AMP (5 mM) or reduced spin-labeled uridine (Alessi et al., 1991) (5 mM) in the perfusate. However, addition of either MgADP (1 mM) or MgATP (1 mM) to the circulating rigor buffer caused complete displacement of the bound MgSL-ADP signal, indicating that MgSL-ADP binds specifically to the active site of myosin in muscle fibers.

The rotational motion of MgSL-ADP bound to the active site of the myosin head was investigated by carrying out experiments with suspensions of myofibrils (Figure 4, bottom) and isolated myosin filaments (Figure 4, top). The use of these randomly oriented samples ensures that spectral narrowing is due entirely to rotational motion, not to orientation (Barnett & Thomas, 1987). The observed spectra are shown on the left, and the spectra on the right have been corrected by subtracting the free SL-ADP signal. With myosin filaments (Figure 4, top right), the hyperfine splitting of 49.0 G indicates that the MgSL-ATP is only moderately immobilized on the protein and still possesses a degree of nanosecond motion independent of the protein to which it is bound. A similar result was found for myofibrils under rigor conditions (Figure 4, bottom right), where the splitting was slightly greater (52.7 G). Thus, the binding of the myosin head to actin only marginally further restricts the degree of immobilization of the nucleotide bound to the crossbridge.

In both cases, the bound SL-ADP signal disappeared when either MgADP (1 mM) or MgATP (1 mM) was added to the incubation buffer but remained unaltered when either AMP (5 mM) or reduced spin-labeled uridine (5 mM) was included.

The results indicate that MgSL-ADP bound to the myosin head has some rotational motion independent of the protein that is slightly altered by binding to actin. Despite the bulky piperidine nitroxyl group anchored to the ribose ring, we have shown that SL-ATP still supports muscle contraction effectively. It may be that the 2′ and 3′ ribose hydroxyl groups of ATP do not make significant restraining contacts with the protein, which accounts for these EPR observations. Thus, the ribose ring of nucleotides bound to the active site of myosin may be free to experience a slight "wobble" and so give rise to the rotational motion seen here.

DISCUSSION

The key step in the synthesis of SL-ATP is the reaction of the enol ether spin-label precursor **1** with AMP. This reaction was previously found to be strongly inhibited by polar organic solvents such as DMF and DMSO (Alessi et al., 1991), probably because the dipolar aprotic solvent reduces the effectiveness of the acid catalyst. We were, therefore, forced in this reaction to use acetonitrile, a nonpolar organic solvent in which AMP is poorly soluble. This accounts for the low yield (20%) for this reaction. Nevertheless, AMP is a convenient starting material to use in this synthesis, first, because the 5′-phosphate group of AMP provides the necessary protection of the 5′-hydroxyl position of adenosine (Alessi et al., 1991) and, second, because the phosphate group readily undergoes pyrophosphorylation to yield the corresponding triphosphate. The synthesis of SL-ATP is also amenable to isotopic labeling of the nitroxyl moiety with ^{15}N and ^{2}H, which would improve the resolution of EPR spectra for orientation

studies (Fajer et al., 1990b). Using the chemistry we have described, relatively large amounts of SL-ATP (400 μmol) are readily obtainable.

As observed in our earlier study (Alessi et al., 1991) the ^{1}H NMR spectra of the *N*-acetoxy intermediates **3** and **4** at room temperature showed that they exist as two conformers, which we believe arise from slowly interconverting conformations of the *N*-acetoxypiperidine ring. The NMR spectrum of the reduced SL-ATP product, however, shows a single set of peaks for each proton, suggesting that the piperidine ring of reduced SL-ATP (and by implication SL-ATP itself) is not in fast conformational exchange. This conclusion is supported by an NMR temperature dependence study of the analogous reduced spin-labeled uridine, which showed that as the temperature was lowered this compound went from fast into intermediate and then into slow exchange (Alessi et al., 1991). A detailed study of model compounds (Anderson & Corrie, 1992) has confirmed these observations and has shown that hindered rotation about the N–O bound in the *N*-acetoxy intermediates **3** and **4** is the principal origin of the barrier to conformational interchange in the piperidine ring.

Our main goals in synthesizing SL-ATP were to study the motion of the myosin cross-bridges in muscle contraction by EPR and to study the cross-bridge structure by NMR. The findings that S1 hydrolyzes SL-ATP and that SL-ATP supports muscle contraction effectively indicate that, when a muscle fiber is contracting with SL-ATP as the substrate, the myosin cross-bridge is going through the same series of intermediates as a fiber contracting with ATP. It is therefore likely that results obtained with SL-ATP as substrate will be relevant to the mechanism of muscle contraction.

The spectrum of SL-ADP, like that of any nitroxide spin label, is potentially sensitive to (1) submicrosecond rotational motion, which averages features of the spectrum in both oriented (e.g., fibers) and unoriented (e.g., myosin solution or myofibril suspension) samples, and (2) orientational order (and disorder) on the microsecond time scale or slower ("static"), which affects the spectrum only in an oriented sample (e.g., fibers). We have recorded spectra from both types of samples to distinguish these two effects, and we find that both effects are present when SL-ADP is bound to myosin. The hyperfine splitting ($2T_\parallel'$) between the two outer peaks of a nitroxyl probe bound to a nonoriented sample such as a solution of myosin filaments or myofibrils (Figure 4) is very sensitive to the rotational motion of the probe on the nanosecond time scale (Hsia & Piette, 1969). A spin-labeled probe strongly immobilized to a large protein such as myosin (with a correlation time of $>10^{-7}$ s) will have a splitting of 66–70 G. The splitting values of 49 and 52.7 G observed for SL-ADP bound to myosin filaments (Figure 4, top) and to myofibrils (Figure 4, bottom), respectively, indicate that the SL-ADP bound to the cross-bridge active site has significant nanosecond rotational motion independent of the myosin head. The order parameter *S*, which describes the angular amplitude of this motion, can be estimated from the expression

$$S = (T_\parallel' - T_0)/(T_\parallel - T_0) \quad (1)$$

where $2T_\parallel'$ is the observed maximum splitting for a randomly oriented sample (illustrated in Figure 4), $2T_\parallel$ is the splitting for an immobile spin label (typically 66–70 G), and $2T_0$ is the isotropic hyperfine splitting for freely tumbling SL-ADP in solution (measured above to be 31.6 G) (Squier & Thomas, 1989). Thus, the order parameters for myosin filaments ($2T_\parallel'$ = 49.0 G) and myofibrils ($2T_\parallel'$ = 52.7 G) are 0.48 ± 0.03 and 0.57 ± 0.02, respectively. One explanation for this observation is that the ribose ring of ADP is not rigidly immobilized at the myosin active site and is therefore free to wobble, resulting in the nitroxyl moiety of SL-ADP having significant rotational motion independent of myosin filaments. If the restricted motion is modeled as a *wobble* within a cone with a half-width θ_c, then

$$\cos \theta_c = -0.5 \pm 0.5*(1 + 8S) \quad (2)$$

(Griffith & Jost, 1976; Thomas, 1986). Thus, the estimated amplitudes for the restricted nanosecond rotation of the spin-label moiety of SL-ADP in the myosin active site are 53 ± 2° and 47 ± 2° for myosin filaments and myofibrils, respectively.

The observation that SL-ATP supports muscle contraction so well indicates that it must be binding to the myosin active site in the same way as ATP. From a survey of the known crystal structures of nucleotide-binding proteins, this is likely to be in a cleft where the ATP is held relatively rigidly with respect to the protein. The ^{31}P NMR data of Shriver and Sykes (1981) appear to uphold this. Furthermore, affinity labeling of myosin with different ATP analogs suggests that all three S1 heavy chain domains may be involved in lining this cleft (Mahmood et al., 1989; Maruta et al., 1989; Okamoto & Yount, 1985). Thus, it may be that ATP binds in a cleft in the S1 head with the 2′,3′ positions of the ribose ring unconstrained and close to the protein's surface. This could explain why 2′(3′)-derived analogs of ATP are such good substrates for myosin [e.g., Cremo et al. (1990) and Woodward et al. (1991)]. Alternatively, we cannot exclude that rapid nitrogen inversion in the piperidine ring of SL-ADP may result in at least some of the observed rotational motion of the bound SL-ADP independent of the myosin head. It should be pointed out, however, that we observed that SL-ATP bound to the CaATPase of the sarcoplasmic reticulum was strongly immobilized (unpublished observations), and it is also worth noting that several commonly used spin-labeled probes containing the six-membered piperidine ring, such as 4-(2-iodoacetamido)-2,2,6,6-tetramethylpiperidinoxyl and 4-maleimido-2,2,6,6-tetramethylpiperidinoxyl, are strongly immobilized (hyperfine splitting ≥68 G) when covalently attached to the myosin head (Thomas et al., 1980; Thomas & Cooke, 1980).

The orientation of myosin heads in a fiber is determined routinely by recording EPR spectra of muscle fiber bundles containing a covalently attached spin-labeled probe with different orientations in the magnetic field (Thomas & Cooke, 1980). Figure 3 shows EPR spectra of SL-ADP bound to myosin heads in rigor oriented parallel and perpendicular to the magnetic field. The large difference between these two spectra indicates that SL-ADP bound to rigor myosin heads is highly oriented relative to the fiber axis. The narrow linewidths of the spectrum of SL-ADP bound to a fiber bundle oriented parallel to the magnetic field are probably due to a combination of the narrow orientational distribution of bound SL-ADP on the myosin head and SL-ADP possessing some nanosecond rotational motion independent of the myosin cross-bridges. Although EPR theory has been developed to analyze oriented EPR spectra, this requires that a spin-labeled probe is strongly immobilized to the protein to which it is attached (Fajer et al., 1990a). The nanosecond mobility of the spin label in the present system prevents the direct application of this theory. To a first approximation, we can assume that the only effect of the rapid motion on the EPR spectra is partially to average the hyperfine interaction tensor values (Griffith & Jost, 1976). The new effective tensor values can be determined

from the spectrum of a randomly oriented sample undergoing the same motion, i.e., the myofibril spectrum in Figure 4 (bottom right). The splitting between the outer extrema gives $2T_{\parallel}' = 52.7$ G, while the splitting between the inner extrema gives $2T_{\perp}' = 22.2$ G. Then for a narrow orientational distribution, the observed splitting for oriented fibers (Figure 3, top right) is given by

$$T'(\theta) = [(T_{\parallel}')^2 \cos^2 \theta + (T_{\perp}')^2 \sin^2 \theta]^{1/2} \quad (3)$$

The observed value of $T'(\theta) = 13.1$ G (Figure 3, top right) gives a value of $\theta = 73.5°$. This is our best estimate for the mean orientation of the principal axis of the spin label relative to the fiber axis.

In the only previous study of nucleotide spin label in muscle, Crowder and Cooke (1987) synthesized and used ATP analogs in which the attachment of the label was to either the 2′ or 3′ position on ribose, in contrast to the present spin label in which both the 2′ and 3′ positions are involved in a more rigid linkage. Despite the difference in spin-label structure, similar EPR results were obtained. Spectra of oriented fibers were consistent with partially oriented spin labels bound to the myosin active site, undergoing restricted nanosecond rotational motion. When spectra of ADP analogs bound to fibers oriented parallel to the field were recorded as in Figure 3 (top left), splittings of about 39 and 29 G were obtained for the 2′ and 3′ analogs, respectively [Figure 5 in Crowder and Cooke (1987)]. These values are greater than the value observed for SL-ADP in the present study (26.15 G), suggesting that our SL-ADP either (a) has its principal axis more perpendicularly oriented or (b) is more rigidly oriented in the myosin active site. However, spectra of randomly oriented myofibrils were not reported in that study, so the degree of nanosecond mobility was not determined and was thus not taken into account when the orientational distributions were analyzed. Thus, a quantitative comparison with the present study, in terms of spin-label mobility or orientational order, is not possible.

In summary, we have established that SL-ADP is a good substrate for actomyosin and for muscle. We have developed EPR methodology for characterizing (and distinguishing) the dynamic (submicrosecond) and static orientation of the spin label when bound to the myosin active site. The large spectral changes induced by fiber reorientation (Figure 3) show that the ribose-bound spin label is highly oriented with respect to the fiber axis. The hyperfine splitting value (less than the rigid limit value) observed in myosin and myofibrils (Figure 4) indicates that the nitroxide moiety undergoes restricted submicrosecond rotational motion when SL-ADP is bound to the myosin active site. This mobility is comparable to that observed previously with other nitroxide spin labels, even though the nitroxide moiety is much more conformationally restricted in this label. This suggests that the rotational freedom observed is representative of the ribose moiety itself, i.e., that ribose has considerable rotational freedom within the myosin active site. The slightly higher splitting observed in myofibrils, compared with that in myosin filaments, suggests that the formation of the rigor bond increases the steric restriction near the ribose moiety. We have also succeeded in developing an assay based on yeast PGK to convert SL-ADP to SL-ATP in muscle fibers. This regenerating system should be applicable to other ribose-modified ATP analogs which are also not substrates for pyruvate kinase or creatine kinase. The regenerating system tested on single muscle fibers was found to be able to relax fibers at concentrations of 250 μM SL-ATP or higher. For the regenerating system to be effective in EPR experiments on bundles of muscle fibers, further experimentation is required to determine the optimal experimental conditions (e.g., concentration of PGK) and to check whether fibers in the core of the bundle behave differently from those on the periphery which benefit from a shorter diffusion path to the surrounding bathing medium. We will then be in a better position to investigate by EPR the orientation and motion of spin-labeled nucleotide bound to myosin cross-bridges in relaxed and contracting muscle fiber bundles. Such experiments are only possible with a recycling system to reduce the signal from the large excess of free SL-ATP that would otherwise be required to achieve relaxation and contraction.

Finally, the chemistry we have described for synthesizing SL-ATP has been used without modification to synthesize the other spin-label ribonucleotides SL-GTP, SL-GDP, SL-CTP, and SL-UTP (unpublished results). We hope that this type of spin-labeled nucleotide in which the motion of the nitroxyl moiety relative to the nucleotide is severely restricted may prove generally useful in the study of the structure and molecular dynamics of many nucleotide-binding proteins which are currently being studied by NMR and EPR.

ACKNOWLEDGMENT

We are grateful to Dr. Neil Baggett for his help during the early phases of this work.

REFERENCES

Alessi, D. R., Corrie, J. E. T., Feeney, J., Trayer, I. P., & Trentham, D. R. (1991) *J. Chem. Soc., Perkin Trans. 1*, 2243–2247.

Anderson, J. E., & Corrie, J. E. T. (1992) *J. Chem. Soc., Perkin Trans. 2*, 1027–1031.

Barany, M., Barnt, K., & Gubba, F. (1957) *Nature (London) 179*, 818–819.

Barnett, V. A., & Thomas, D. D. (1987) *Biochemistry 26*, 314–323.

Brenner, B., & Eisenberg, E. (1986) *Proc. Natl. Acad. Sci. U.S.A. 83*, 3542–3546.

Cremo, C. R., Neuron, J. M., & Yount, R. G. (1990) *Biochemistry 29*, 3309–3319.

Crowder, M., & Cooke, R. (1987) *Biophys. J. 51*, 323–333.

Eastwood, A. B., Wood, D. S., Bock, K. L., & Sorenson, M. M. (1979) *Tissue Cell 11*, 553–566.

Edman, K. A. P. (1979) *J. Physiol. 291*, 143–159.

Fajer, P. G., Fajer, E. A., Brunsvold, E. A., & Thomas, D. D. (1988) *Biophys. J. 53*, 513–524.

Fajer, P. G., Bennett, R. L. H., Polnaszek, C. F., Fajer, E. A., & Thomas, D. D. (1990a) *J. Magn. Reson. 88*, 111–125.

Fajer, P. G., Fajer, E. A., Matta, J. J., & Thomas, D. D. (1990b) *Biochemistry 29*, 5865–5871.

Ferenczi, M. A. (1986) *Biophys. J. 50*, 471–477.

Ferenczi, M. A., Homsher, E., & Trentham, D. R. (1984) *J. Physiol. 352*, 575–599.

Fiske, C. H., & Subbarow, Y. (1925) *J. Biol. Chem. 66*, 375–400.

Ford, L. E., Huxley, A. F., & Simmons, R. M. (1977) *J. Physiol. 269*, 441–515.

Froehler, B. C., & Matteucci, M. D. (1983) *Nucleic Acids Res. 11*, 8031–8036.

Furfine, C. S., & Velick, S. F. (1965) *J. Biol. Chem. 240*, 844–855.

Goldman, Y. E., & Simmons, R. M. (1984) *J. Physiol. 350*, 497–518.

Griffith, O. H., & Jost, P. C. (1976) in *Spin Labeling: Theory and Applications* (Berliner, L. J., Ed.) pp 453–523, Academic Press, New York.

Hampton, A., & Slotin, L. A. (1975) *Biochemistry 14*, 5438–5444.

Hanes, C. S. (1932) *Biochem. J. 26*, 1406–1421.
Hiratsuka, T. (1983) *Biochim. Biophys. Acta 742*, 496–508.
Hoard, D. E., & Ott, D. G. (1965) *J. Am. Chem. Soc. 87*, 1785–1788.
Hsia, J. C., & Piette, L. H. (1969) *Arch. Biochem. Biophys. 129*, 296–307.
Huxley, A. F., & Simmons, R. M. (1971) *Nature (London) 233*, 533–538.
Kosen, P. A. (1989) *Methods Enzymol. 89*, 86–121.
Krietsch, W. K. G., & Bücher, T. (1970) *Eur. J. Biochem. 17*, 568–580.
Leatherbarrow, R. J., Fersht, A. R., & Winter, G. (1985) *Proc. Natl. Acad. Sci. U.S.A. 82*, 7840–7844.
Lehninger, A. L. (1970) in *Biochemistry*, Chapter 15, Worth Publishers, New York.
Maeda, M., Patel, A. D., & Hampton, A. (1977) *Nucleic Acids Res. 4*, 2843–2853.
Mahmood, R., Elizinga, M., & Yount, R. G. (1989) *Biochemistry 28*, 3989–3995.
Mannherz, H. G., Schenck, H., & Goody, R. S. (1974) *Eur. J. Biochem. 46*, 287–295.
Margossian, S. S., & Lowey, S. (1982) *Methods Enzymol. 85*, 55–58.
Maruta, S., Miyanishi, T., & Matsuda, G. (1989) *Eur. J. Biochem. 184*, 213–221.
Okamoto, Y., & Yount, R. G. (1985) *Proc. Natl. Acad. Sci. U.S.A. 82*, 1575–1579.
Roberts, G. C. K., Hannah, J., & Jardetsky, O. (1969) *Science 165*, 504–505.
Seidel, J. C. (1982) *Methods Enzymol. 85*, 594–624.
Shriver, J. W., & Sykes, B. D. (1981) *Biochemistry 20*, 6357–6362.
Spudich, J. A., & Watt, S. (1971) *J. Biol. Chem. 246*, 4866–4871.
Squier, T. C., & Thomas, D. D. (1989) *Biophys. J. 56*, 735–748.
Thomas, D. D. (1986) in *Techniques for the Analysis of Membrane Proteins* (Cherry, R. J., & Ragan, I., Eds.) pp 377–431, Chapman and Hall, London.
Thomas, D. D. (1987) *Annu. Rev. Physiol. 49*, 691–709.
Thomas, D. D., & Cooke, R. (1980) *Biophys. J. 32*, 891–906.
Thomas, D. D., Ishiwata, S., Seidel, J. C., & Gergely, J. (1980) *Biophys. J. 32*, 873–890.
Trayer, H. R., & Trayer, I. P. (1988) *Biochemistry 27*, 5718–5727.
Trentham, D. R. (1971) *Biochem. J. 122*, 59–69.
Trentham, D. R., Bardsley, R. G., Eccleston, J. F., & Weeds, A. G. (1972) *Biochem. J. 126*, 635–644.
Wagner, P. D., Slater, C. S., Pope, B., & Weeds, A. G. (1979) *Eur. J. Biochem. 99*, 385–394.
Walker, J. W., Reid, G. P., & Trentham, D. R. (1989) *Methods Enzymol. 172*, 290–301.
Webb, M. R. (1992) *Proc. Natl. Acad. Sci. U.S.A. 89*, 4884–4887.
Woodward, S. K. A., Eccleston, J. F., & Geeves, M. A. (1991) *Biochemistry 30*, 422–430.